Drug Delivery

DOI: 10.1002/ange.201408510

A Preloaded Amorphous Calcium Carbonate/Doxorubicin@Silica Nanoreactor for pH-Responsive Delivery of an Anticancer Drug**

Yang Zhao, Zhong Luo, Menghuan Li, Qiuyu Qu, Xing Ma, Shu-Hong Yu, and Yanli Zhao**

Abstract: *Biomedical applications of nontoxic amorphous calcium carbonate (ACC) nanoparticles have mainly been restricted because of their aqueous instability. To improve their stability in physiological environments while retaining their pH-responsiveness, a novel nanoreactor of ACC–doxorubicin (DOX)@silica was developed for drug delivery for use in cancer therapy. As a result of its rationally engineered structure, this nanoreactor maintains a low drug leakage in physiological and lysosomal/endosomal environments, and responds specifically to pH 6.5 to release the drug. This unique ACC–DOX@silica nanoreactor releases DOX precisely in the weakly acidic microenvironment of cancer cells and results in efficient cell death, thus showing its great potential as a desirable chemotherapeutic nanosystem for cancer therapy.*

Calcium carbonate ($CaCO_3$), as a naturally nontoxic biomineral, shows great potential for biomedical applications, with intrinsic advantages of degradability at certain pH values, biocompatibility, simple chemical composition, as well as low cost and ease of large-scale production. To date, crystallized $CaCO_3$ has been widely used as a successful carrier for the delivery of drugs, genes, and proteins.[1] However, the main problem of its micrometer size limits its application in nanomedicine. In contrast to the crystallized form, amorphous calcium carbonate (ACC) can be readily obtained on a nanoscale.[2] We have utilized monodispersed ACC nanoparticles as templates to prepare a preloaded drug-delivery carrier and theranostic system for biomedical application.[3] However, the high aqueous instability of ACC,[4] including its ease of dissolution and phase transition, has limited the development of pH-responsive nanomedicine directly based on ACC nanoparticles.

To overcome this challenge, the concept of a nanoreactor was introduced for the design of a pH-responsive drug-delivery nanosystem. According to the typical core–shell structure of a nanoreactor,[5] this system should thus consist of an ACC–drug core and a permeable shell. The permeable shell should protect the ACC–drug core from unexpected drug leakage. In addition, this shell should specifically allow an acidic stimulus to initiate the interior reactions for drug release. To meet these demands, we herein describe the fabrication of an amorphous calcium carbonate/doxorubicin@silica (ACC–DOX@silica) nanoreactor. In this design, the acidic stimulus, controlled by the silica shell, could trigger the inner reactions in the ACC–DOX core. After dissociating from the core, the protonated DOX molecule would adhere to the negatively charged silica shell through a pH-dependent electrostatic attraction instead of being released directly, thus allowing a sustained cancer treatment.

As shown in Figure 1, the ACC–DOX@silica nanoreactor was obtained in two steps, including the self-assembly of a preloaded ACC–DOX core and surface coating with a silica shell. In the first step, uniform and monodispersed ACC–DOX nanoparticles (purple, left inset image in Figure 1 A) with a diameter of around 130 nm (Figure 1 B) were prepared in one step by a vapor-diffusion process. These nanoparticles contain a DOX weight percentage of up to 5.9%. UV/Vis spectroscopy was utilized to investigate the interaction between the DOX and Ca^{2+} (see Figure S1 in the Supporting Information). The addition of DOX to the solution of $CaCl_2$ in ethanol resulted in the UV/Vis spectra showing the same characteristic band as that of pure DOX. During the vapor diffusion process, ammonia was generated from ammonium bicarbonate, which then dissolved in the ethanol solution. The solution became purple, and the absorption band of DOX

[*] Dr. Y. Zhao, Dr. Z. Luo, Q. Qu, X. Ma, Prof. Y. L. Zhao
Division of Chemistry and Biological Chemistry
School of Physical and Mathematical Sciences
Nanyang Technological University
21 Nanyang Link, Singapore 637371 (Singapore)
E-mail: zhaoyanli@ntu.edu.sg
Homepage: http://www.ntu.edu.sg/home/zhaoyanli/
M. Li, Prof. Y. L. Zhao
School of Materials Science and Engineering
Nanyang Technological University
Singapore 639798 (Singapore)
Prof. S.-H. Yu
Division of Nanomaterials and Chemistry
Hefei National Laboratory for Physical Sciences at Microscale
Department of Chemistry
University of Science and Technology of China
Hefei, Anhui 230026 (P.R. China)
E-mail: shyu@ustc.edu.cn
Homepage: http://staff.ustc.edu.cn/~yulab/

[**] Y.L.Z. acknowledges funding support from the National Research Foundation (NRF), Prime Minister's Office, Singapore, under its NRF Fellowship (NRF2009NRF-RF001-015), Campus for Research Excellence and Technological Enterprise (CREATE) Programme-Singapore Peking University Research Centre for a Sustainable Low-Carbon Future, and the NTU-A*Star Centre of Excellence for Silicon Technologies (A*Star SERC No. 112 351 0003). S.-H.Y. acknowledges funding support from the National Basic Research Program of China (Grants 2010CB934700, 2013CB933900, 2014CB931800) and the National Natural Science Foundation of China (Grants 21431006, 91022032, 91227103).

Supporting information for this article is available on the WWW under http://dx.doi.org/10.1002/anie.201408510.

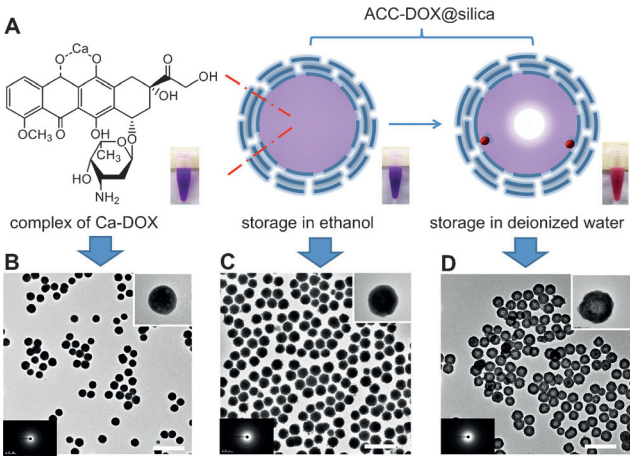

Figure 1. A) Schematic representation of the ACC–DOX@silica nanoreactor and its stability in ethanol and water. Insert images (from left to right) are the suspensions of ACC–DOX in ethanol, ACC–DOX@silica in ethanol, and ACC–DOX@silica in water. Representative TEM images of B) ACC–DOX nanoparticles in ethanol, C) ACC–DOX@silica in ethanol, and D) ACC–DOX@silica in water. The scale bars are 500 nm. Insert images in (B)–(D) are the enlarged TEM images and electron diffraction images.

red-shifted from 480 nm to 550 nm and finally to 590 nm. Based on previous reports on the formation of complexes between DOX and transition metals in alkaline media,[6] it could be concluded that DOX chelated with Ca^{2+} during the synthetic process, and finally was encapsulated in the nanoparticles in the form of a Ca–DOX complex (Figure 1 A). Such a complex in the ACC–DOX nanoparticles exhibited high stability in ethanol solution without any drug leakage (see Figure S2 in the Supporting Information). When the ACC–DOX nanoparticles were suspended in aqueous solution (aqueous buffers of pH 7.4, 6.5, and 5.5, as well as diluted HCl solution), the resulting orange solutions showed the characteristic absorption band of DOX at 480 nm (see Figures S1 and S3 in the Supporting Information), which suggests that the DOX dissociated from the Ca–DOX complex in the aqueous environment. The release profiles of the pH-responsive ACC–DOX nanoparticles were investigated under various pH conditions. A burst release of DOX was observed not only under acidic conditions of pH 6.5 and 5.5, but also at a physiological value of pH 7.4 (see Figure S2 in the Supporting Information). The release behavior could be explained by the water-induced dissolution/phase transition and acid-induced decomposition of the ACC nanoparticles in aqueous environments.[7] The DOX dissociated from the nanoparticles and reformed as free drug molecules during the decomposition of the ACC nanoparticles.

In the second step, the silica shell was introduced to prevent the water-induced dissolution of the ACC–DOX nanoparticles, while retaining its pH-responsiveness for drug delivery. The permeability of the silica shell was optimized (see Figure S4 in the Supporting Information). The amorphous phase of the optimized ACC–DOX@silica nanoparticles (Figure 1 D) in aqueous suspension was characterized by electron diffraction studies. The FTIR spectrum showed the characteristic splitting bands of ACC at 1417 and 1474 cm^{-1} (see Figure S5 in the Supporting Information).[2c] The morphological differences between ACC–DOX@silica nanoparticles in alcoholic and aqueous suspensions (Figure 1 C,D) were monitored by chemical mapping (see Figure S6 in the Supporting Information) of the distributions of N and Ca, which represent DOX and ACC, respectively. The DOX molecules were homogeneously distributed in the core of the ACC–DOX@silica nanoparticles when suspended in ethanol. After transferring the nanoparticles into water, the DOX and ACC vanished from the center and a cavity was formed in the nanoparticles, thereby suggesting partial dissolution of the ACC–DOX core in an aqueous environment. More interestingly, as shown in Figure 2 A, such ACC–DOX@silica nanoparticles exhibited an extremely low leakage of DOX (less than 3%) at pH 7.4 at room temperature, thus indicating a high stability in a physiological environment.

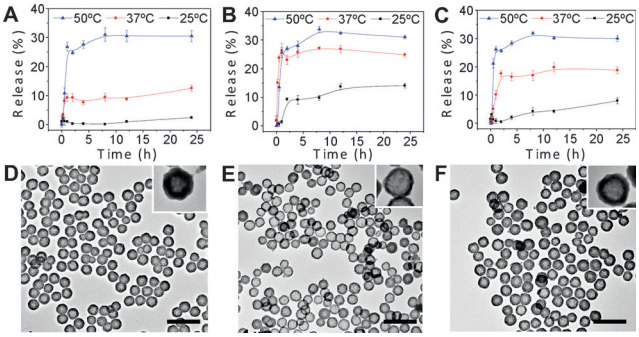

Figure 2. Cumulative releases of DOX from ACC–DOX@silica suspensions in various aqueous buffers at A) pH 7.4, B) pH 6.5, and C) pH 5.5 with different temperatures of 25, 37 and 50 °C. Representative TEM images of the suspensions under 37 °C at D) pH 7.4, E) pH 6.5, and F) pH 5.5. The scale bars are 500 nm.

As a stimulus-triggered drug-delivery system, the pH-responsive release of DOX is pivotal for the application of the ACC–DOX@silica nanoreactor. Therefore, cumulative release profiles were investigated at predetermined temperatures in a series of buffers of pH 7.4, 6.5, and 5.5, which mimicked the microenvironments of healthy tissue, tumor tissue, and cellular lysosomes, respectively.[8] As shown in Figure 2 A–C, the highest percentage drug release at room temperature (25 °C) and physiological temperature (37 °C) was observed at pH 6.5, rather than at pH 7.4 or 5.5. The representative morphologies of the samples at 25 °C (see Figure S7 in the Supporting Information) and 37 °C (Figure 2 D–F) at various pH values precisely reflected the same trend. When the temperature was increased to 50 °C, the release profiles at the three pH conditions were very similar. This distinctive pH-responsiveness could be explained by the well-engineered design of the ACC–DOX@silica nanoreactor. The core–shell structure means that two steps are involved in the escape of DOX: 1) DOX dissociates from the Ca–DOX complex by water-induced dissolution and an acid-induced decomposition of the ACC–DOX core. The intake of water and acid is mediated by the permeability of the silica shell. 2) DOX passes through the silica shell and

enters into the external environment. In this step, the status of the dissociated DOX could affect its interaction with the silica shell.

DOX, with a pK_a of 8.2,[9] is positively charged at pH 7.4, 6.5, and 5.5. The ACC–DOX@silica nanoparticles were negatively charged between pH 7.4 and pH 5.0 (see Figure S8 in the Supporting Information). This means that, under all the pH conditions used for drug release, there are electrostatic attractions between the positively charged DOX[10] and negatively charged silanol groups,[11] which could hamper the escape of DOX and lower the permeability of the silica shell.[12] Therefore, H^+ could serve two functions during the drug release: it could facilitate the dissociation of DOX from the ACC–DOX core to accelerate drug release or it could enhance the electrostatic interaction between the DOX and silica shell by increasing the degree of protonation[13] of DOX, thereby decreasing the drug release. As a result, cumulative drug release from the ACC–DOX@silica nanoreactor would not simply be increased or decreased in response to changes in the pH value from 7.4 to 5.5. At 25 °C and 37 °C, the mutual constraint of the twofold function of the pH stimulus led to the highest cumulative release of DOX at pH 6.5. In addition to the pH stimulus, the permeability of a poorly condensed silica shell could be enhanced by increasing the temperature,[12] which is the reason for the temperature-responsive release of DOX from this nanoreactor. At 50 °C, the highly increased permeability of the silica shell dominates the drug-release process, and thus the drug–release profile is independent of the pH value.

The extraordinary pH-responsiveness (see Figures S9 and S10 in the Supporting Information) of this ACC–DOX@silica nanoreactor makes it capable of carrying out specific drug release in the weakly acidic microenvironment of around pH 6.5 in tumor cells. As expected, the nanoreactor showed a low drug leakage at a physiological pH 7.4 and endosomal/lysosomal pH 5.5, thus suggesting a great potential to reduce the side effects of chemotherapy and to protect drugs from inactivation by the harmful environment. In addition, the characteristic absorption band of the DOX released under these conditions (see Figure S11 in the Supporting Information) shifted back to 480 nm, thus confirming that the DOX molecule was intact after the release.

The feasibility of the pH-responsive ACC–DOX@silica nanoparticles for delivery of an anticancer drug was evaluated using HeLa cells. Firstly, the performance of free DOX and ACC–DOX@silica nanoparticles was investigated in vitro. To mimic the weakly acidic microenvironment in a tumor, ACC–DOX@silica nanoparticles were presuspended in a cell culture medium at pH 6.5 and 37 °C for 2 h before coculturing with cells. As shown in Figure 3 A–C, after coculturing for 1 h, most of the free DOX rapidly concentrated in the nucleus area, which is consistent with previous reports.[14] In contrast, when encapsulated in the ACC–DOX@silica nanoparticles, the DOX is immobilized and cannot freely enter the nucleus unless it is released as a free drug. In the case of ACC–DOX@silica nanoparticles at pH 7.4, most of DOX was retained within the nanoparticles in cytoplasm (Figure 3 D–F). However, after the pretreatment at pH 6.5, DOX was specifically released from the nanoreactor and found in nuclei

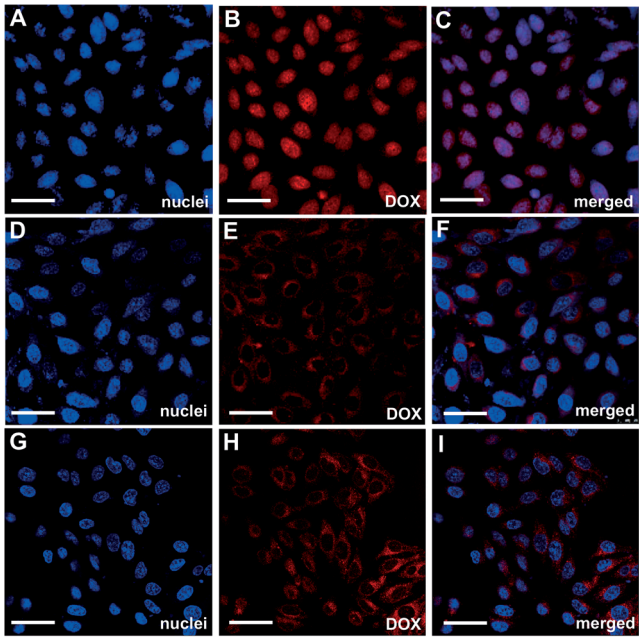

Figure 3. Confocal laser scanning microscopy (CLSM) images of HeLa cells cocultured with native DOX (A–C), ACC–DOX@silica nanoparticles at pH 7.4 (D–F), and ACC–DOX@silica nanoparticles at pH 6.5 (G–I) after 1 h. For the samples at pH 6.5, ACC–DOX@silica nanoparticles were presuspended with cell culture media at pH 6.5 and 37 °C for 2 h before coculturing with cells. The images in the left column are the nuclei stained with Hoechst 33258 (blue), the images in middle column are with DOX (red), and the images in right column are merged images from the left and middle columns. The scale bars are 50 μm.

(Figure 3 G–I). These results indicate that the ACC–DOX@silica nanoparticles are capable of specifically responding to the pathological microenvironment in a pH-responsive manner for drug release.

To compare the cancer-cell killing effects, free DOX and ACC–DOX@silica were investigated in terms of cell viability over 5 days. Without the DOX drug, the ACC@silica carrier exhibited very low cytotoxicity, even after 5 days (Figure 4 A). In the case of free DOX, fast intercalation into the DNA base pairs in nuclei[15] led to rapid cell-killing effects (Figure 4 B). In contrast, the pH-responsiveness of the ACC–DOX@silica nanoparticles after uptake by cells determines the sustained killing effects in the intracellular physiological environment. As observed from the CLSM images of HeLa cells cultured from 1 h to 3 days (Figure 4 D and see Figure S12 in the Supporting Information), the amount of DOX released from the ACC–DOX@silica nanoparticles slightly increased in the nuclei. On the other hand, deformed nuclei induced by the cytotoxicity of the released DOX emerged after an incubation for 6 h. Since the cytotoxicity of the DOX accumulated as the amount released increased, significant cell death was observed on the third day. Consequently, the cell viability after treatment with these nanoparticles showed a typical time-dependent cell death (Figure 4 C). Furthermore, an analogous therapeutic effect of the ability of ACC–DOX@silica nanoparticles to release DOX on the fifth day confirmed the adequate cell-killing capability of this nanoreactor.

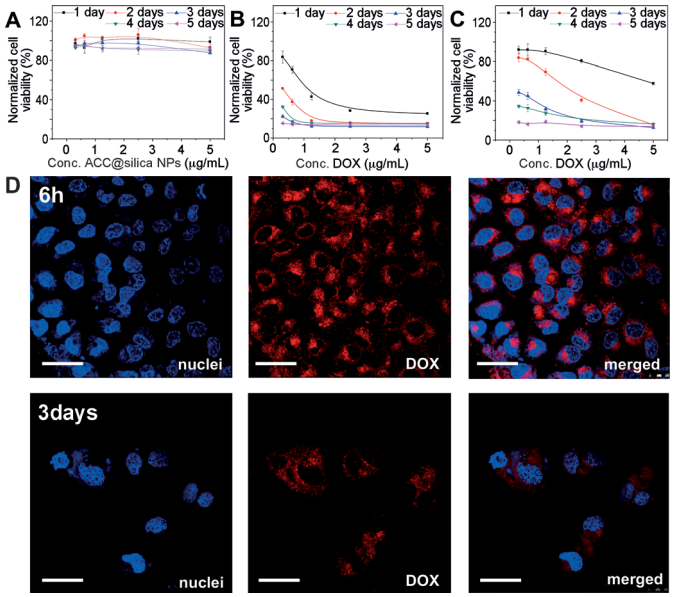

Figure 4. Cell viability of HeLa cells cocultured with A) ACC@silica nanoparticles, B) DOX, and C) ACC–DOX@silica nanoparticles after various periods of 1–5 days. The samples were all at pH 7.4. D) CLSM images of HeLa cells cocultured with the ACC–DOX@silica nanoparticles after 6 h and 3 days. The images in the left column are the nuclei stained with Hoechst 33258 (blue), the images in middle column are with DOX (red), and the images in the right column are merged images from the left and middle columns. The scale bars are 50 μm.

In conclusion, an ACC–DOX@silica nanoreactor with precise pH-responsiveness for drug release has been developed. As a consequence of the rationally engineered structure, this nanoreactor could selectively release the drug at pH 6.5. This feature of the nanoreactor facilitates the specific drug release in the weakly acidic microenvironment of a tumor, thereby leading to an efficient tumor-cell killing effect in a sustained manner. Thus, the nanoreactor has a great potential for cancer therapy.

Received: August 25, 2014
Revised: October 31, 2014
Published online: November 24, 2014

Keywords: amorphous calcium carbonate · antitumor agents · doxorubicin · drug delivery · medicinal chemistry

[1] a) S. Kim, C. B. Park, *Adv. Funct. Mater.* **2013**, *23*, 10–25; b) D. V. Volodkin, R. von Klitzing, H. Möhwald, *Angew. Chem. Int. Ed.* **2010**, *49*, 9258–9261; *Angew. Chem.* **2010**, *122*, 9444–9447; c) W. Wei, G. H. Ma, G. Hu, D. Yu, T. McLeish, Z. G. Su, Z. Y. Shen, *J. Am. Chem. Soc.* **2008**, *130*, 15808–15810; d) Y. Zhao, Y. Lu, Y. Hu, J.-P. Li, L. Dong, L.-N. Lin, S.-H. Yu, *Small* **2010**, *6*, 2436–2442.

[2] a) G. B. Cai, G. X. Zhao, X. K. Wang, S. H. Yu, *J. Phys. Chem. C* **2010**, *114*, 12948–12954; b) H. Fukano, T. Takahashi, M. Aizawa, H. Yoshimura, *Inorg. Chem.* **2011**, *50*, 6526–6532; c) S. F. Chen, H. Colfen, M. Antonietti, S. H. Yu, *Chem. Commun.* **2013**, *49*, 9564–9566.

[3] a) Y. Zhao, L. N. Lin, Y. Lu, S. F. Chen, L. Dong, S. H. Yu, *Adv. Mater.* **2010**, *22*, 5255–5259; b) Y. Zhao, L.-N. Lin, Y. Lu, H.-L. Gao, S.-F. Chen, P. Yang, S.-H. Yu, *Adv. Healthcare Mater.* **2012**, *1*, 327–331.

[4] a) L. Addadi, S. Raz, S. Weiner, *Adv. Mater.* **2003**, *15*, 959–970; b) J. Ihli, Y. Y. Kim, E. H. Noel, F. C. Meldrum, *Adv. Funct. Mater.* **2013**, *23*, 1575–1585.

[5] a) M. A. Mahmoud, R. Narayanan, M. A. El-Sayed, *Acc. Chem. Res.* **2013**, *46*, 1795–1805; b) C. G. Palivan, O. Fischer-Onaca, M. Delcea, F. Itel, W. Meier, *Chem. Soc. Rev.* **2012**, *41*, 2800–2823; c) A. Ranquin, W. Versees, W. Meier, J. Steyaert, G. P. Van, *Nano Lett.* **2005**, *5*, 2220–2224; d) Q. Yan, J. Wang, Y. Yin, J. Yuan, *Angew. Chem. Int. Ed.* **2013**, *52*, 5070–5073; *Angew. Chem.* **2013**, *125*, 5174–5177.

[6] a) B. C. L. Cheung, T. H. T. Sun, J. M. Leenhouts, P. R. Cullis, *Biochim. Biophys. Acta Biomembr.* **1998**, *1414*, 205–216; b) G. N. C. Chiu, S. A. Abraham, L. M. Ickenstein, R. Ng, G. Karlsson, K. Edwards, E. K. Wasan, M. B. Bally, *J. Controlled Release* **2005**, *104*, 271–288; c) H. Drechsel, M. Fiallo, A. Garnier-Suillerot, B. F. Matzanke, V. Schunemann, *Inorg. Chem.* **2001**, *40*, 5324–5333; d) Y. Chen, Y. Wan, Y. Wang, H. J. Zhang, Z. J. Jiao, *Int. J. Nanomed.* **2011**, *6*, 2321–2326; e) Y. X. Deng, H. J. Zhang, *Int. J. Nanomed.* **2013**, *8*, 1835–1841.

[7] M. Kellermeier, E. Melero-Garcia, F. Glaab, R. Klein, M. Drechsler, R. Rachel, J. M. Garcia-Ruiz, W. Kunz, *J. Am. Chem. Soc.* **2010**, *132*, 17859–17866.

[8] a) J. Madsen, I. Canton, N. J. Warren, E. Themistou, A. Blanazs, B. Ustbas, X. Tian, R. Pearson, G. Battaglia, A. L. Lewis, S. P. Armes, *J. Am. Chem. Soc.* **2013**, *135*, 14863–14870; b) Y. Li, J. Wang, M. G. Wientjes, J. L. Au, *Adv. Drug Delivery Rev.* **2012**, *64*, 29–39; c) J. T. Wilson, S. Keller, M. J. Manganiello, C. Cheng, C. C. Lee, C. Opara, A. Convertine, P. S. Stayton, *ACS Nano* **2013**, *7*, 3912–3925; d) Y. Wang, K. Zhou, G. Huang, C. Hensley, X. Huang, X. Ma, T. Zhao, B. D. Sumer, R. J. Deberardinis, J. Gao, *Nat. Mater.* **2014**, *13*, 204–212.

[9] H. A. Meng, M. Liong, T. A. Xia, Z. X. Li, Z. X. Ji, J. I. Zink, A. E. Nel, *ACS Nano* **2010**, *4*, 4539–4550.

[10] S. K. Sahu, S. K. Mallick, S. Santra, T. K. Maiti, S. K. Ghosh, P. Pramanik, *J. Mater. Sci. Mater. Med.* **2010**, *21*, 1587–1597.

[11] a) J. Liu, W. Bu, L. Pan, J. Shi, *Angew. Chem. Int. Ed.* **2013**, *52*, 4375–4379; *Angew. Chem.* **2013**, *125*, 4471–4475; b) M. Sulpizi, M.-P. Gaigeot, M. Sprik, *J. Chem. Theory Comput.* **2012**, *8*, 1037–1047; c) K. Leung, I. M. B. Nielsen, L. J. Criscenti, *J. Am. Chem. Soc.* **2009**, *131*, 18358–18365.

[12] Y. Hu, Q. Zhang, J. Goebl, T. Zhang, Y. Yin, *Phys. Chem. Chem. Phys.* **2010**, *12*, 11836–11842.

[13] a) Y. C. Huang, M. Arham, J. S. Jan, *Eur. Polym. J.* **2013**, *49*, 726–737; b) A. Z. Mirza, H. Shamshad, *Eur. J. Med. Chem.* **2011**, *46*, 1857–1860.

[14] a) M. J. Kirchmeier, T. Ishida, J. Chevrette, T. M. Allen, *J. Liposome Res.* **2001**, *11*, 15–29; b) E. C. R. Roti, S. K. Leisman, D. H. Abbott, S. M. Salih, *PLoS One* **2012**, *7*, e42293.

[15] a) P. M. Peiris, L. Bauer, R. Toy, E. Tran, J. Pansky, E. Doolittle, E. Schmidt, E. Hayden, A. Mayer, R. A. Keri, M. A. Griswold, E. Karathanasis, *ACS Nano* **2012**, *6*, 4157–4168; b) S. Barua, S. Mitragotri, *ACS Nano* **2013**, *7*, 9558–9570.